THE ASTROPHYSICAL JOURNAL, 459:271–277, 1996 March 1

THE EFFECT OF DEEP HYDROGEN BURNING IN THE ACCRETED ENVELOPE OF A NEUTRON STAR ON THE PROPERTIES OF X-RAY BURSTS

RONALD E. TAAM
Department of Physics and Astronomy, Northwestern University, Evanston, IL 60208; taam@ossenu.astro.nwu.edu

S. E. WOOSLEY
UCO/Lick Observatory, Board of Studies in Astronomy and Astrophysics, University of California, Santa Cruz, CA 95064; General Studies Group, Physics Department L298, Lawrence Livermore National Laboratory, P.O. Box 808, Livermore, CA 94550; woosley@lick.ucsc.edu

AND

D. Q. LAMB
Department of Astronomy and Astrophysics, University of Chicago, 5640 South Ellis Avenue, Chicago, IL 60637; lamb@pion.uchicago.edu

Received 1995 July 17; accepted 1995 September 7

ABSTRACT

The thermal and compositional evolution of a neutron star has been numerically followed to determine the long-term properties of X-ray bursts produced by thermonuclear shell flashes in its accreted hydrogen-rich envelope. Uniform burning over the entire neutron star surface is assumed and mass accretion rates greater than $\sim 0.1 \dot{M}_{\rm Edd}$ (where $\dot{M}_{\rm Edd}$ is the critical mass accretion rate for which the accretion luminosity is equal to the Eddington luminosity) are considered. Specific attention is focused on the consequences of electron capture initiated burning of hydrogen at high densities ($\gtrsim 10^7$ g cm^{-3}). The degree of heating associated with the burning of the residual hydrogen (i.e., the matter which is not completely processed in the outburst) is a function of the mass accretion rate and the composition of the accreted matter. Heating of the neutron star envelope is found to be more important for greater mass accretion rates and for greater residual hydrogen abundances. Because of the higher envelope temperatures, the resulting bursts are weaker and recur more frequently, for a given mass accretion rate, than in situations where the deep hydrogen burning does not occur.

The mass accretion rate, which delineates strong X-ray bursts (where the ratio of the peak burst luminosity to the quiescent level of emission is greater than ~ 3) from weak X-ray bursts, lies in the range of 0.1–0.2 times the Eddington value. Weak burst activity is found for accretion rates extending to about the Eddington limit provided that the helium content of the accreted matter is greater than ~ 0.23. The implications of our results with regard to the absence of regular, periodic X-ray bursting activity in the bright low-mass X-ray binary sources are briefly discussed.

Subject headings: nuclear reactions, nucleosynthesis, abundances — stars: interiors — stars: neutron — X-rays: bursts

1. INTRODUCTION

The thermonuclear flash model for the type I X-ray burst phenomenon provides a natural explanation for the global properties (i.e., peak luminosities $\sim 10^{38}$ ergs s^{-1}, energies $\sim 10^{39}$ ergs, rise time ~ 1 s, and intervals of roughly hours) of the observed bursts. Although the general characteristics of X-ray bursts are explicable in terms of thermonuclear flashes in the envelope of an accreting neutron star, the lack of a quantitative understanding of the more detailed observational data implies that the theoretical description is incomplete. A comprehensive review of the observations and the theoretical status of the X-ray burst phenomenon is given in a recent paper by Lewin, van Paradijs, & Taam (1993).

With a view toward achieving the goal of using X-ray burst theory to constrain the fundamental properties of the X-ray source, recent theoretical studies of the X-ray burst phenomenon have focused on the evolution of a neutron star undergoing a series of thermonuclear flashes in its accreted envelope. The investigations of Fushiki et al. (1992) and Taam et al. (1993), following the earlier work of Fujimoto et al. (1985) and Woosley & Weaver (1985), have advanced the theory of the X-ray burst phenomenon beyond the simple picture originally proposed by Woosley & Taam (1976) (see also Joss 1977; Lamb & Lamb 1978) by taking account of the thermal and compositional history of the accreted envelope. For example, the lack of correlation between the time intervals between bursts and the persistent level of emission seen in some burst sources (e.g., Ser X-1, Li et al. 1977; 1735 − 44, Lewin et al. 1980; 1608 − 522, Murakami et al. 1980; EXO 0748 − 67, Gottwald et al. 1986) may be explicable and can now be explained in terms of the effects of thermal history of the neutron star envelope without requiring a variation in the mass accretion rate, provided that the core of the neutron star is cool ($T \lesssim 10^8$ K) and the abundance of the accreted material is metal poor ($Z \lesssim 0.001$). In addition, the appearance of weak bursts with peak luminosities of ~ 0.1–0.2 times the Eddington limit and recurrence timescales less than 2 hr, as observed from EXO 0748 − 67 (Gottwald et al. 1986), and the energetics of the bursts from MXB 1636 − 536 (Fujimoto et al. 1987) were also difficult to understand within the framework of the simple model. It is now believed that these properties are a direct consequence of the compositional history of the neutron star envelope. In particular, these weak bursts result from the burning of the residual nuclear fuel from previous outbursts linked to the inward transport of helium to high densities via a Rayleigh-Taylor mixing instability (see Taam et al. 1993).

From the early works of Ayasli & Joss (1982), Fujimoto et al. (1985), and Woosley & Weaver (1985), it is known that the hydrogen is not completely burned out in the outburst and that some residual hydrogen remains. That hydrogen is not completely burned during the outburst is due to the fact that hydrogen burning involves weak interactions and, at the relevant conditions in the neutron star envelope, these reactions are necessarily slower than the charged particles reactions involving helium nuclei. Eventually this hydrogen will be converted to heavier elements as a result of electron capture processes at high densities ($\gtrsim 10^7$ g cm^{-3}). Fushiki et al. (1992) make use of the energy available from this source to provide an explanation for the long decay timescales (~ 2500 s) of an X-ray burst emitted from Aql X-1 (Czerny, Czerny, & Grindlay 1987). In their model, the long X-ray tail is associated only with the first X-ray burst emitted during the transient outburst. In this paper we extend our earlier studies to focus on the long-term consequences of the deep hydrogen burning on the properties of the emitted X-ray bursts. This study is complementary to our more recent work (Taam et al. 1993), where we examined the thermal and compositional evolution of the neutron star in response to successive thermonuclear shell flashes for moderate to low mass accretion rates. Here, we examine the moderate to high mass accretion rate range (i.e., $\dot{M} \gtrsim 0.1\dot{M}_{\rm Edd}$, where $\dot{M}_{\rm Edd}$ is the mass accretion rate for which the accretion driven luminosity is equal to the Eddington luminosity) where the effects of deep hydrogen burning on the thermal structure of the neutron star are of much greater importance.

Sources which exhibit very irregular burst behavior, such as Cyg X-2 and GX 17+2 (Kahn & Grindlay 1982; Kuulkers et al. 1994, 1995b), and sources which show a lack of detectable bursts, such as Sco X-1, GX 5−1, and GX 340−0, at high persistent luminosities (van Paradijs, Pennix, & Lewin 1988) may be undergoing such a phase of nuclear burning. We point out that the conclusion that the accretion rates in these systems are very high is not straightforward since the relationship between the mass accretion rate and the persistent level of emission can be complicated, for example, by the anisotropy of the radiation field during the burst active and inactive periods (see Lewin et al. 1993). Nevertheless, previous studies either indicate that bursting activity extends above the Eddington mass accretion rate (see Fushiki 1986 for the steady state approximation) or can cease below the Eddington limit (Ayasli & Joss 1982) for a neutron star of a sufficiently high envelope temperature ($\sim 6 \times 10^8$ K) accreting at a low rate ($\sim 0.01\dot{M}_{\rm Edd}$). The envelope temperatures required for suppression of strong, regular X-ray bursts at the higher mass accretion rates suggested by the observations of these sources have not been determined. That is, the relationship between the envelope temperature of the neutron star and the mass accretion rate near the Eddington limit remains to be established. In neither of these studies was the effect of deep hydrogen burning considered. In the next section we describe the results of our long-term time-dependent calculations for a range of mass accretion rates and compositions of the accreted matter. The implications of the results to the observed properties of X-ray bursts are discussed in the last section with particular emphasis on the very bright low-mass X-ray binary systems.

2. RESULTS

The evolution of the neutron star envelope was followed with a version of the KEPLER computer program (Weaver, Zimmerman, & Woosley 1978) that has been modified to treat nuclear fusion on the surfaces of accreting neutron stars (see Woosley & Weaver 1985). Specifically, the code includes implicit hydrodynamics; continuous rezoning; an equation of state that describes the contributions of ions, radiation, electrons, and pairs of arbitrary degree of degeneracy; electron scattering opacity and electron conduction; a diffusive model for semiconvection based on a mixing length formulation; and a nuclear reaction network. The nuclear energy is generated by the rapid proton capture process (see Wallace & Woosley 1981), α captures on intermediate-mass nuclei, and electron capture onto hydrogen at high densities (see below). To treat the accretion of matter, we vary the surface pressure until the pressure reaches a characteristic value whereupon a new mass zone is added. At this point the temperature, density, and velocity of the new zone is assumed to be the same as the zone immediately below. Thereafter, the boundary pressure is reset to zero, and the calculation continues. For a more complete description of the numerical technique, see Woosley & Weaver (1985). For the purposes of this study we have further modified the code to include general relativistic effects as described in Thorne (1977), which have been implemented in the manner outlined in Ayasli & Joss (1982). In particular, it is assumed that the gravitational redshift correction factors are constant throughout the envelope since the variation of the radial coordinate is small compared to the radius of the neutron star. This approximation should be adequate provided that the envelope does not expand significantly in response to the thermonuclear outburst. Since we are primarily interested in the moderate to high mass accretion rate regime where the X-ray bursts are expected to be weak, this approximation should be adequate. Following our earlier work, we also assume that the nuclear burning is uniform over the entire stellar surface. The initial models were constructed in thermal equilibrium and included the outer $10^{-8}\ M_\odot$ of the neutron star envelope corresponding to densities and temperatures ranging up to $\sim 2 \times 10^9$ g cm^{-3} and 1.16×10^8 K. The mass and radius of the neutron star are chosen to be 1.4 $M_\odot$ and 9.1 km, respectively.

The parameters characterizing each of the model sequences include the hydrogen and CNO metal abundance of the accreted matter, X and $Z_{\rm CNO}$, and the mass accretion rate, $\dot{M}$, in units of the Eddington value. For convenience, these parameters are listed for each sequence in Table 1. The results of the numerical calculations are summarized in

TABLE 1
INITIAL PARAMETERS OF X-RAY BURST SEQUENCES

Sequence	X	$Z_{\rm CNO}$	$\dot{M}(\dot{M}_{\rm Edd})$
1	0.70	0.001	0.9500
2	0.70	0.020	0.9500
3	0.75	0.020	0.9500
4	0.70	0.001	0.4750
5	0.70	0.020	0.4750
6	0.70	0.001	0.2375
7	0.70	0.020	0.2375
8	0.70	0.001	0.1060
9	0.70	0.020	0.1060

TABLE 2

PROPERTIES OF X-RAY BURST SEQUENCES

Sequence	X_r	T_{env} (10^8 K)	Δt (minutes)	γ
1	0.083	7.98	10	1.08
2	0.076	8.07	8	1.07
3	0.217	9.19	...	...
4	0.080	7.58	19	1.20
5	0.080	7.48	19	1.21
6	0.182	6.95	36–40	1.47
7	0.089	6.08	59–62	1.89
8	0.137	5.58	60–132	1.6–2.9
9	0.041	4.52	96–233	2.4–4.7

Table 2. Here, we list some characteristics of the neutron star envelope, viz., the residual hydrogen abundance at the base of the hydrogen-helium burning layer, X_r, and the maximum temperature near the base of the hydrogen layer, T_{env}. In addition, we also list the recurrence time, Δt, and the ratio of the bolometric value of the peak luminosity to the persistent level of emission, γ, of the resulting X-ray burst.

To investigate the nuclear burning behavior of the neutron star envelope at mass accretion rates near the Eddington value we calculated sequences 1–3 in which the mass accretion rate was chosen to be $0.95\dot{M}_{Edd}$. Each of these sequences is distinguished by the composition of the accreted matter. In the following we first describe the evolutionary history of sequence 1 corresponding to a composition of $X = 0.7$ and $Z_{CNO} = 0.001$. After an initial phase during which the envelope was heated by a succession of thermonuclear flashes (see Taam et al. 1993), deep hydrogen burning became important when the densities exceeded $\sim 10^7$ g cm^{-3} (corresponding to an amount of accreted mass exceeding $\sim 10^{23}$ g). At these high densities, electron capture occurs via the $p(e^-, \nu)n$ reaction since the Fermi energy of the electrons is greater than the rest mass energy difference between a neutron and a proton. Hence, hydrogen burning proceeds, starting with the series of reactions $p(n, \gamma)^2$H$(p, \gamma)^3$He (^{3}He, $2p$)^{4}He and extending up to ^{56}Ni. As a result of the high residual hydrogen abundance (~ 0.3) the hydrogen burning luminosity raised the temperatures to a maximum of 1.1×10^9 K at a density of 2.4×10^7 g cm^{-3}. Consequently, the bursting activity ceased in the outer 10^{21} g of the envelope where helium is present since the temperature sensitivity of the helium burning rates is weakened at the temperatures (6×10^8 K) characteristic of these regions. However, as a result of these high temperatures and densities ($\sim 10^6$ g cm^{-3}) in this region, the residual hydrogen abundance decreased. Thus, the hydrogen burning luminosity and the envelope temperatures correspondingly decreased, leading to the resumption of weak bursting activity in the outer envelope. After ~ 6.4 days of evolution the thermal structure in the deep interior approached an asymptotic state. At this time the residual hydrogen abundance had been reduced to 0.083 and the temperatures, which had been raised from $\sim 5 \times 10^8$ K (prior to deep hydrogen burning) to 1.1×10^9 K, declined to 8×10^8 K. This evolution illustrates the operation of a feedback process that leads to a significant decrease in the residual hydrogen abundance below that present in the absence of a deep hydrogen burning phase at high mass accretion rates near the Eddington limit. As indicated above, the nuclear burning in the hydrogen-helium layer returns to instability because the temperature sensitivity of the triple α reaction is still high at the relevant temperatures in this region ($\sim 4.5 \times 10^8$ K). The unstable burning behavior in the hydrogen-rich layer containing helium follows from the triple α reaction coupled with the break-out from the CNO cycle via the ^{14}O(α, p)^{17}F and ^{15}O(α, γ)^{19}Ne reactions (see Wallace & Woosley 1981; Taam 1985). The nature of these thin shells confirms results by Fujimoto, Hanawa, & Miyaji (1981) and Fushiki & Lamb (1987) based on the local and nonlocal linear analyses, respectively. The resulting X-ray bursts are weak, as the ratio of the net peak burst luminosity to the persistent accretion driven luminosity is 0.08, have long rise times of ~ 25 s, last for ~ 3 minutes, and recur rapidly on timescales of 10 minutes (see Fig. 1). The long rise timescale indicates that hydrogen burning is significantly contributing to the energy production during the outburst. These properties differ from those bursts emitted prior to deep hydrogen burning where the bursts are stronger (with the net peak burst luminosity larger by a factor of 3.5), reflecting a longer recurrence timescale (~ 28 minutes).

In model sequence 2, we consider the accretion of matter that has a solar-like metal composition (i.e., $Z_{CNO} = 0.02$). As can be gleaned from Table 2 the results of the evolution are quantitatively similar to those of sequence 1. This insensitivity to the CNO abundance in the accreted matter stems from the fact that, at these high rates of mass accretion, significant CNO nuclei are produced via the triple α and proton capture reactions. As a result, the properties of the emitted X-ray bursts do not differ significantly from those of sequence 1.

On the other hand, the thermal and nuclear evolution of the neutron star envelope is very sensitive to the helium abundance in the accreted matter. This is illustrated by model sequence 3, in which the helium abundance has been reduced from 0.28 in sequence 2 to 0.23. In this sequence, the actual mass accretion rate is lower by a factor of 0.97 because of the dependence of the Eddington mass accretion rate on the composition of the accreted matter. In this case, the final residual abundance of hydrogen has increased by nearly a factor of 3 to 0.22. Because of the higher residual

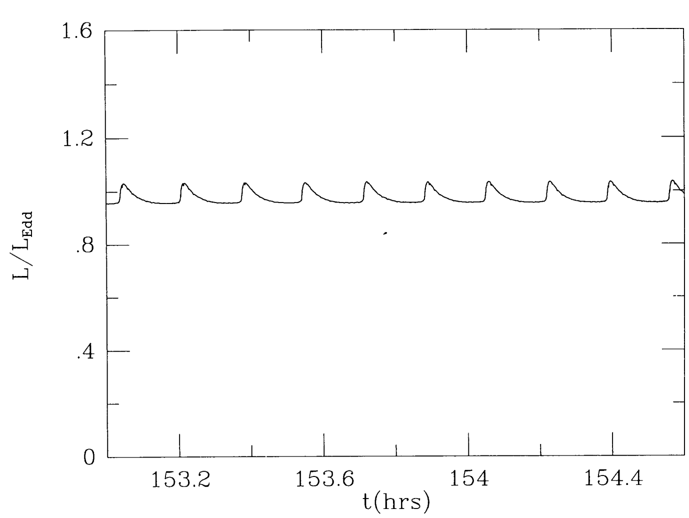

FIG. 1.—The bolometric light curve from an accreting neutron star (including the contribution due to accretion) in sequence 1 during the late phase of evolution when deep hydrogen burning takes place. The luminosity is expressed in terms of the Eddington limit, and the timescales are measured in hours. Note that the light curve is very regular, which indicates that the source has approached a limiting cyclic state.

hydrogen abundance, the hydrogen burning luminosity generated in the deep interior is increased, and hence the temperatures are elevated to a greater degree. In particular, the maximum temperatures in the accreted hydrogen layer are raised to a 9.19×10^8 K. In this evolution, the temperature at the base of the hydrogen-helium burning layer is increased to 5.6×10^8 K, which is sufficient to reduce the temperature sensitivity of the triple α burning rate to render the layer thermally stable. In this case, the nuclear burning is steady and its contribution to the total luminosity is $\sim 3\%$.

To determine the dependence of the thermal and compositional structure of the neutron star interior and its affect on the X-ray burst properties with respect to the mass accretion rate, the rate was decreased by a factor of 2 to $0.475\dot{M}_{\rm Edd}$ in sequences 4 and 5. After the thermal transient phase associated with the bursting activity prior to the onset of deep hydrogen burning, the results are similar to those of sequences 1 and 2 in the sense that the results are not sensitive to the CNO abundances of the accreted matter. In particular, the residual hydrogen abundance remains at ~ 0.08. However, the nuclear luminosity associated with deep hydrogen burning is reduced because of the lower mass accretion rate, and this leads to lower envelope temperatures near the base of the hydrogen layer of $\sim 7.5 \times 10^8$ K (in comparison to 8×10^8 K in sequence 1). The properties of the resulting X-ray bursts directly reflect these lower temperatures. Specifically, the recurrence timescale increases by nearly a factor of 2 to ~ 19 minutes and the ratio of peak burst luminosity to quiescent luminosity increases to 1.2 (see Table 2).

In model sequences 6 and 7, the mass accretion rate is further reduced by another factor of 2 to $0.2375\dot{M}_{\rm Edd}$. For this rate of mass accretion the maximum envelope temperature at the base of the layer containing residual hydrogen is reduced to 6.95×10^8 K and 6.08×10^8 K for sequences 6 and 7, respectively. Thus, the trends established from sequences 1, 2, 4, and 5 are reaffirmed. The lower envelope temperatures lead to stronger outbursts (see below). In fact, in contrast to the previous sequences, convection is important in transporting energy during the thermonuclear flash. In addition to these differences, the results do depend on the initial CNO abundances of the accreted material. In particular, the residual hydrogen abundances are lower for a higher CNO metal abundance (see Table 2). The dependence of the residual hydrogen abundance on the mass accretion rate follows from the fact that the temperatures in the outer 10^{21} g are lower than the corresponding region of the neutron star for the higher mass accretion rates characterizing sequences 1–5. As a result, there is less nuclear processing of the CNO nuclei in the accreted layer in comparison to sequences characterized by higher mass accretion rates. Consequently, less hydrogen is consumed in the outburst and the effects of deep hydrogen burning are more important for the sequence corresponding to $Z_{\rm CNO} = 0.001$, where $X_r = 0.18$, than to the sequence corresponding to $Z_{\rm CNO} = 0.02$, where $X_r = 0.089$. As a result, the temperatures in the deep hydrogen layer are correspondingly higher for sequence 6 than for sequence 7. The light curves for sequences 6 and 7 are shown in Figures 2 and 3, respectively. It can be seen that the sequence characterized by the higher initial metallicity emits X-ray bursts that are stronger. In addition, these bursts recur less frequently (because of the lower envelope temperatures) than the sequence characterized by a low initial metallicity. In both cases, the light curves are distinguished by their regularity, which implies that a limit cycle has been nearly reached. Following the trends from the sequences at higher mass accretion rates, the recurrence timescale of the outburst increases by about another factor of 2 to 36–40 minutes for sequence 6 and by more than a factor of 2 to 59–62 minutes for sequence 7, and the ratio of peak burst luminosity to persistent level of emission increases to 1.47–1.89. The ratio of the persistent luminosity to the time-averaged burst emission (averaged over the time interval prior to the burst), denoted as α, is fairly constant from burst to burst and averages ~ 77 for the bursts in Figure 2 and ~ 63 for the bursts in Figure 3.

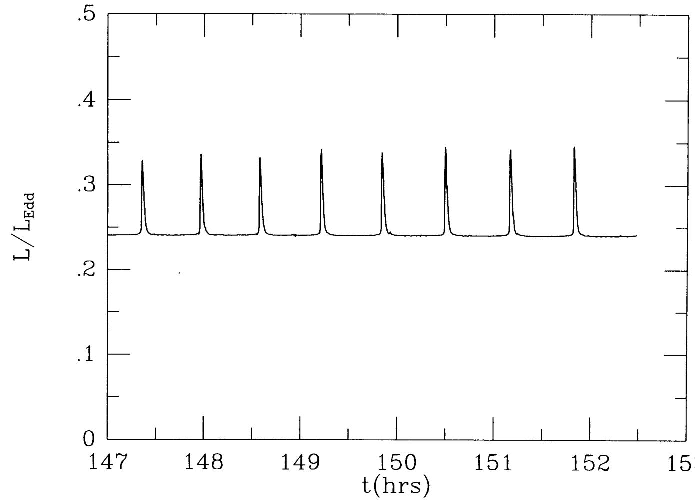

FIG. 2.—The temporal bolometric luminosity variations from the neutron star (including the contribution due to accretion) in sequence 6. The luminosity is in units of the Eddington limit, and the timescales are expressed in hours. The contribution of nuclear fusion to the total luminosity is greater than in Fig. 1. The light curve remains regular.

To further explore the transition between strong and weak X-ray burst behavior, we carried out calculations at the lowest mass accretion rates considered in this study ($0.106\dot{M}_{\rm Edd}$) for model sequences 8 and 9. In these sequences, the envelope cools to a greater extent than in previous sequences because of the longer mass accretion timescale. Here the envelope temperatures near the base of

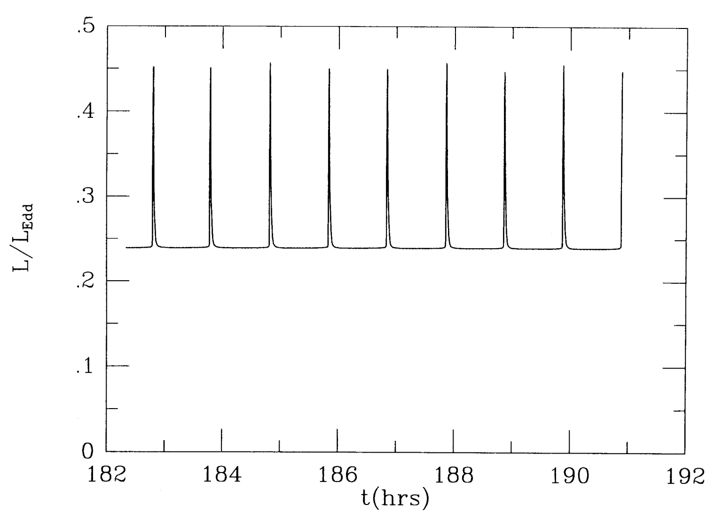

FIG. 3.—The luminosity profile for sequence 7. The light curve is similar to the profile for sequence 6. The regularity of the light curve does not depend on the initial CNO abundance of the accreted matter.

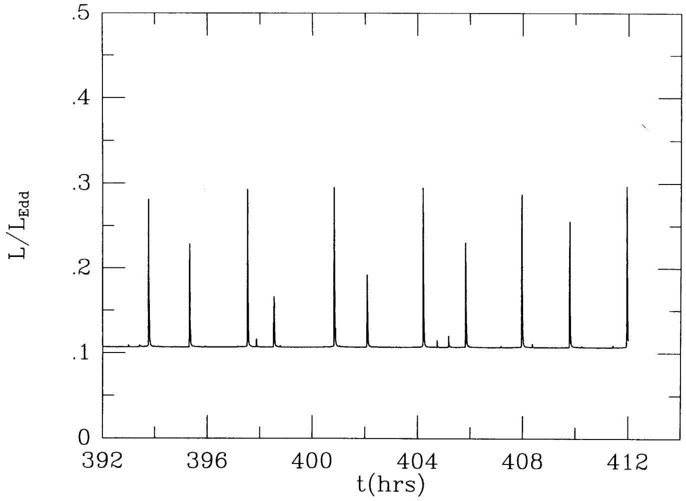

FIG. 4.—Same as in Fig. 1, but for sequence 8. Note the light curve differs from the previous sequences. The burst behavior is irregular with the recurrence time and peak burst luminosity varying between individual bursts.

the hydrogen layer are $\sim 5.6 \times 10^8$ K and $\sim 4.5 \times 10^8$ K for sequences 8 and 9, respectively. These temperatures should be regarded as indicative for this choice of mass accretion rate since the asymptotic state has not been reached. The thermal state evolves continuously in response to the bursting activity in the outer surface layers. Because of the lower envelope temperatures, the thermonuclear flash takes place at a higher degree of electron degeneracy, and the emitted X-ray bursts are stronger, but characterized by luminosities still less than the Eddington limit. These bursts also occur less frequently with much less regularity than in the previous sequences. This property is illustrated in the light curves for each of the sequences in Figures 4 and 5. It can be seen that the stronger bursts occur after a longer waiting time. In both sequences, the occurrence of bursting activity is irregular, ranging from ~ 1 to 2.2 hr for sequence 8 and from ~ 1.6 to 3.8 hr for sequence 9. Upon comparison of these sequences with sequences 6 and 7, we note that the recurrence timescale does not have a simple scaling relationship with the mass accretion rate. For example, if one assumes that the recurrence timescale is only inversely proportional to the mass accretion rate, then the timescale is expected to be in the range of 80–90 minutes for sequence 8. The fact that the range in recurrence timescale for sequence 8 is wider than this estimate indicates that the amount of mass necessary to initiate the thermal instability varies. The longer recurrence timescales for sequence 9 reflect the lower envelope temperatures in the deep interior. In comparison with sequence 8, this is a consequence of the fact that the residual hydrogen abundance is so low (i.e., nearly all the accreted matter is burned in the outburst since $X_r = 0.04$) that burning of this hydrogen does not lead to significant heating of the deep interior. As a result, sequence 9 corresponds to the case when the heating associated with deep hydrogen burning is minimal. The increase in ratio of the peak burst luminosity to the quiescent level of emission, γ, in comparison with sequences at higher mass accretion rates reflects not only the decrease in the level in the persistent emission, but also to an increase in the peak burst luminosity. The α values are found to vary from 83 to 159 with an average value of 114 for the bursts in Figure 4. On the other hand, α ranges from 70 to 118 with an average value of 92 for the bursts in Figure 5. The smaller values of α in sequence 9 reflect the more complete combustion of nuclear fuel associated with a greater initial CNO abundance in the accreted matter. These values are larger than those found for sequences 6 and 7 at higher rates of mass accretion. This indicates that a smaller fraction of the nuclear energy is emitted in the form of the X-ray burst for these lower mass accretion rates, with a greater fraction of the nuclear energy conducted into the core. The continually evolving thermal state of the interior in the sequences characterized by the low mass accretion rates reflects this inward energy flow.

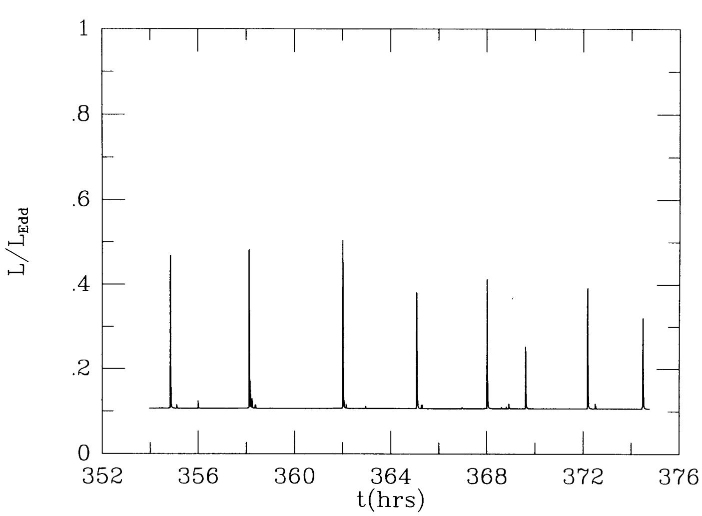

FIG. 5.—Same as in Fig. 1, but for sequence 9. The irregular burst behavior is similar to that seen in Fig. 4 and indicates that this type of activity extends over a wide range of the initial CNO abundances in the accreted matter.

3. DISCUSSION

In this paper, we have examined the effects of the residual hydrogen resulting from the incomplete processing of accreted matter in a thermonuclear flash on the long-term thermal and compositional evolution of a neutron star. It is found that the burning of this hydrogen, initiated by electron capture reactions, leads to additional heating of the neutron star interior. Its effect is significant, and its importance increases with higher rates of mass accretion. The thermal and compositional state of the accreted neutron star envelope is modified in the sense that it is hotter and the residual hydrogen abundance in mass layers beneath the hydrogen-helium burning layer is lower in comparison to numerical models in which the effects of deep hydrogen burning are not included. This leads to X-ray bursts that are weaker and to bursts that recur more frequently. The results indicate that electron capture initiated hydrogen burning reactions should be included in investigations of the long-term evolution of the accreted envelope for mass accretion rates in excess of $\sim 0.1\dot{M}_{\rm Edd}$. For rates below this value or for the early stages of an outburst of a soft X-ray transient (when the mass accretion rate is near the Eddington value, but the base of the hydrogen layer is located at densities $\lesssim 10^7$ g cm^{-3}), deep hydrogen burning is unimportant.

We have found that strong X-ray bursts (where the ratio of the peak burst luminosity to the accretion driven luminosity is $\gtrsim 3$) are produced by the nuclear outburst for mass accretion rates $\lesssim 0.1\dot{M}_{\rm Edd}$. The strength of the outburst is correlated with the CNO abundances of the accreted matter. More energetic bursts result from the accretion of matter characterized by higher metallicities. The burst behavior is found to be irregular, with recurrence times ranging over a factor of 2, at a constant rate of mass accretion, which confirms and extends our earlier work on the shorter term evolution of a neutron star (Fushiki et al. 1992; Taam et al. 1993) accreting at lower rates. Such irregular behavior reflects the effects of the thermal and compositional inertia of the neutron star on the properties of the X-ray bursts (see Taam 1980; Woosley & Weaver 1985). In contrast to the behavior of the neutron star accreting at lower mass accretion rates ($\dot{M} \lesssim 0.04\dot{M}_{\rm Edd}$), there is no evidence of a phase of weak X-ray burst activity initiated by the convective mixing mechanism associated with the Rayleigh-Taylor instability (Taam et al. 1993). The results of the present paper suggest that the mixing mechanism that results from the inversion of the mean molecular weight is sufficiently vigorous to produce premature ignition only at lower mass accretion rates. This is in accordance with the findings of Taam et al. (1993), in which it was found that the convective mixing mechanism is less effective for envelopes characterized by higher internal temperatures.

Our results preclude the possibility for strong bursts for accretion rates $\gtrsim 0.1\dot{M}_{\rm Edd}$ provided that the composition of the accreted matter is hydrogen rich. For the accretion of very helium rich matter, the above limit does not apply since the lack of significant hydrogen burning necessarily leads to lower envelope temperatures and to stronger outbursts. This is likely to be the case in MXB 1820−30 (Stella, Priedhorsky, & White 1987a). The existence of strong bursts in MXB 1820−30 (Haberl et al. 1987) and the interpretation that its mass accretion rate is greater than $0.1\dot{M}_{\rm Edd}$ (Nobili, Turolla, & Lapidus 1994; Lapidus, Nobili, & Turolla 1994) based on the radiatively driven wind model is generally consistent with this expectation. However, it should be pointed out that the mass accretion rates inferred from this model are very sensitive to the observational determination of the minimum and maximum color temperatures during the expansion phase of the burst.

It has also been found that the X-ray bursting activity extends to at least $0.95\dot{M}_{\rm Edd}$ provided that the helium abundance in the neutron star envelope is $\gtrsim 0.23$. The existence of bursts (identified to be of thermonuclear origin) from the very bright low-mass X-ray binary system, GX 17+2 (Tawara et al. 1984; Sztajno et al. 1986; Kuulkers et al. 1994, 1995a) provides support for this theoretical result. In this source, the X-ray bursts emitted are weak (reaching maximum intensity of ∼30%–40% of the persistent flux level), last for a time ranging from 1 to 5 minutes, and are observed infrequently. In addition, GX 17+2 is also a *Z* source in the X-ray color-color diagram (see van der Klis 1995 for a recent review), and it exhibits quasi-periodic oscillations at ∼24–28 Hz on the horizontal branch (Hasinger 1987) and at ∼7 Hz on the normal branch (Stella, White, & Priedhorsky 1987b). The theoretical understanding of the oscillations on the normal branch in terms of a radiation instability in a quasi-spherical accretion flow (Fortner, Lamb, & Miller 1989; Miller & Lamb 1992) or as a variation in the vertical structure of an accretion disk (Alpar et al. 1992) indicates that GX 17+2 accretes at rates near the Eddington limit in this spectral state. The flux enhancements characteristic of these calculated bursts near the Eddington mass accretion rate are small, and they may not always be detectable against the fairly large brightness fluctuations of these sources. Hence, only the largest bursts would be identified as bursts. Given the fact that the mass accretion rates in the *Z* sources are thought to vary by a factor of 2, the equilibrium burning regions are generally not in compositional or thermal equilibrium with the instantaneous mass accretion rate. This departure from a limiting cyclic state may help explain the observation of several bursts that produced flux enhancements of ∼1.4 when the accretion rate was near $\dot{M}_{\rm Edd}$.

Sources such as Sco X-1, GX 5−1, and GX 340−0 do not exhibit bursting behavior, and this suggests that either mass accretion rate variations on timescales of minutes mask these intrinsic variations or that the physical conditions under which nuclear burning takes place may be modified by other effects. Among the various possibilities for the latter interpretation include the circumstance that the envelope of the neutron star is hotter than that determined by the nuclear burning in the accreted layers resulting in smaller intrinsic fluctuations. This is unlikely since the neutron stars in systems with low-mass evolved companions (e.g., Sco X-1) are not expected to be young. Another possibility is to invoke that the composition of the accreted matter differs from that of the accreting matter. For example, the helium and CNO abundances in the neutron star envelope may be lower than that transferred by its companion due to the spallation processes in an accretion shock (Bildsten, Salpeter, & Wasserman 1992, 1993). This effect is a stronger possibility since for the rates of mass accretion considered in this study the matter may flow in quasi-spherically (see Fortner et al. 1989), rather than in the equatorial plane via an accretion disk. In this case, the energy of the infalling ions is greater since the gas flows to the neutron star surface at nearly the free-fall velocity. However, the spallation reactions are inhibited at accretion rates close to the Eddington value since the effective gravity is lowered, thereby reducing the incident kinetic energy of the ions. Although Bildsten et al. (1993) claim that the helium reforms in the neutron star envelope, it is not excluded that the helium abundance in the accreted layer is less than that in the transferred matter from the companion. Finally, it is possible that the assumption of a spherically symmetric outburst is not realized at high rates of mass accretion. The relaxation of the spherical approximation for the ignition and propagation of the burning front is perhaps a more promising explanation for the lack of strong X-ray bursting activity in these sources. For a neutron star with a pure helium envelope, the work of Bildsten (1994) indicates that the propagation time of the burning wave can be longer than the thermal diffusion timescale to the surface as long as the nuclear energy is transported by radiation rather than by convection. In the models studied in this paper, convective energy transport is important during the thermonuclear flash for bursts characterized by net peak luminosities $\gtrsim 0.1$ times the Eddington limit. This occurs at mass accretion rates $\lesssim 0.24\dot{M}_{\rm Edd}$. For mass accretion rates greater than this critical value, the nuclear energy is primarily transported by radiative processes, and it would follow that the burning could be spatially localized. Provided that the spatial extent of the unstable region is sufficiently small compared to the radius of the neutron star, the outbursts would be barely perceptible above the quiescent level of emission. This is not inconsistent with the observations that indicate that bursting activity ceases for accretion rates of $\sim 0.3\dot{M}_{\rm Edd}$ (van Paradijs et al. 1988).

Although the multidimensionality of the outburst is an attractive explanation for the burst inactivity, the existence of bursts in GX 17+2 while on the normal branch (see Kuulkers et al. 1994, 1995a; also Kahn & Grindlay 1984) suggests that the physical conditions in the accreted neutron star envelope must occasionally differ from its non-burst state and from the other bright low-mass X-ray sources at mass accretion rates near the Eddington limit so that the burst can be seen above the quiescent level of emission. Within the framework of the multidimensional model for X-ray bursts, the propagation speed of the burning front around the neutron star surface or the thermal diffusion timescale to the neutron star surface must be increased so that the spatial extent of the burning region is not constrained to a small fraction of the neutron star surface. Future investigations of the propagation of burning fronts in a hydrogen-rich environment at mass accretion rates near the Eddington limit will be necessary to determine the viability of such a hypothesis.

This research has been supported in part by NASA under grants NAGW-830, NAGW-1284, NAGW-2525, and NAGW-2526, by NSF under grant AST 9115367, and at LLNL by the Department of Energy under grant W-7405-ENG-48. We thank F. Lamb and D. Psaltis for their comments.

REFERENCES

Alpar, M. A., Hasinger, G., Shaham, J., & Yancopoulos, S. 1992, A&A, 257, 627
Ayasli, S., & Joss, P. C. 1982, ApJ, 256, 637
Bildsten, L. 1994, ApJ, 418, L21
Bildsten, L, Salpeter, E. E., & Wasserman, I. 1992, ApJ, 384, 183
———. 1993, ApJ, 408, 615
Czerny, M., Czerny, B., & Grindlay, J. E. 1987, ApJ, 312, 122
Fortner, B, Lamb, F. K., & Miller, G. S. 1989, Nature, 342, 775
Fujimoto, M. Y., Hanawa, T., Iben, I. Jr., & Richardson, M. B. 1985, in High Energy Transients in Astrophysics, ed. S. E. Woosley (New York: AIP), 302
Fujimoto, M. Y., Hanawa, T., & Miyaji, S. 1981, ApJ, 247, 267
Fujimoto, M. Y., Sztanjo, M., Lewin, W. H. G., & van Paradijs, J. 1987, ApJ, 319, 902
Fushiki, I. 1986, Ph.D. thesis, Harvard Univ.
Fushiki, I., & Lamb, D. Q. 1987, ApJ, 323, L55
Fushiki, I., Taam, R. E., Woosley, S. E., & Lamb, D. Q. 1992, ApJ, 390, 634
Gottwald, M., Haberl, F., Parmar, A., & White, N. E. 1986, ApJ, 308, 213
Haberl, F., Stella, L., White, N. E., Priedhorsky, W. C., & Gottwald, M. 1987, ApJ, 314, 266
Hasinger, G. 1987, A&A, 186, 153
Joss, P. C. 1977, Nature, 270, 310
Kahn, S. M., & Grindlay, J. E. 1982, ApJ, 281, 821
Kuulkers, E., van der Klis, M., Oosterbroek, T., van Paradijs, J., & Lewin, W. 1994, in The Evolution of X-ray Binaries, ed. S. S. Holt & C. S. Day (New York: AIP), 539
———. 1995a, preprint
Kuulkers, E., van der Klis, M., & van Paradijs, J. 1995b, ApJ, 450, 748
Lamb, D. Q., & Lamb, F. K. 1978, ApJ, 220, 291
Lapidus, I., Nobili, L., & Turolla, R. 1994, ApJ, 433, 287
Lewin, W. H. G., van Paradijs, J., Cominsky, L, & Holzner, S. 1980, MNRAS, 193, 15
Lewin, W. H. G., van Paradijs, J., & Taam, R. E. 1993, Space Sci. Rev., 62, 223
Li, F. K., Lewin, W. H. G., Clark, G. W., Doty, J., Hoffman, J. A., & Rappaport, S. A. 1977, MNRAS, 179, 21p
Miller, G. S., & Lamb, F. K. 1992, ApJ, 388, 541
Murakami, T., et al. 1980, ApJ, 240, L143
Nobili, L., Turolla, R., & Lapidus, I. 1994, ApJ, 433, 276
Stella, L., Priedhorsky, W., & White, N. E. 1987, ApJ, 312, L17
Stella, L., White, N. E., & Priedhorsky, W. 1987, ApJ, 315, L49
Sztajno, M., van Paradijs, J., Lewin, W. H. G., Langmeier, A., Trumper, J., & Pietsch, W. 1986, MNRAS, 222, 499
Taam, R. E. 1980, ApJ, 241, 351
———. 1985, Annu. Rev. Nucl. Part. Sci., 35, 1
Taam, R. E., Woosley, S. E., Weaver, T. A., & Lamb, D. Q. 1993, ApJ, 413, 324
Tawara, Y., Hirano, T., Kii, T., Matsuoka, M., & Murakami, T. 1984, PASJ, 36, 861
Thorne, K. S. 1977, ApJ, 212, 825
van der Klis, M. 1995, in X-Ray Binaries, ed. W. H. G. Lewin, J. van Paradijs, & E. P. J. van den Heuvel (Cambridge: Cambridge Univ. Press), 252
van Paradijs, J., Penninx, W., & Lewin, W. H. G. 1988, MNRAS, 233, 437
Wallace, R. K., & Woosley, S. E. 1981, ApJS, 43, 389
Weaver, T. A., Zimmerman, G. B., & Woosley, S. E. 1978, ApJ, 225, 1021
Woosley, S. E., & Taam, R. E. 1976, Nature, 263, 101
Woosley, S. E., & Weaver, T. A. 1985, in High Energy Transients in Astrophysics, ed. S. E. Woosley (New York: AIP), 273